PERGAMON

International Journal of Rock Mechanics and Mining Sciences 36 (1999) 119–126

International Journal of
Rock Mechanics
and Mining Sciences

Technical Note

On the thermal degradation of marble

G.F. Royer-Carfagni

Dipartimento di Ingegneria Civile, Università di Parma, Viale delle Scienze, Parma 43100, Italy

Accepted 4 August 1998

1. Introduction

In modern usage, the word marble has a very wide range of meanings and is often used to refer to any of those rocks, regardless of origin, usually employed in the building industry for pavements or coverings. The present paper deals with marble as defined in its strict sense: the quasi-monomineral metamorphic rock made up of an aggregate of calcite (calcium carbonate) crystal granules. The varieties of marble are distinguished, rather than by appreciable differences in mineral composition, by the mosaic texture of their constituent grains, which may range between the two extreme cases termed "*homoblastic*" and "*xenoblastic*", schematically represented in Fig. 1. The first is composed of regular-shaped grains with straight or gently curving boundaries, such as the Pentelic marble used by the Athenians to build the Parthenon. The second, peculiar to some varieties quarried in Carrara, is characterized by the interlacing of irregular crystals closely fitting along their wavy contours.

The degradation of marble, clearly evident in many historical monuments, typically consists of the progressive loosening of rock cohesion and manifests itself by increased porosity and a tendency to crumble. Among the many possible causes of marble decay, an important role is played by temperature changes, hence the term "*marmo cotto*" (i.e. "baked marble") used for centuries by quarrymen in Carrara to denote any marble presenting poor mechanical properties. This same term was introduced into the scientific literature by Lord Rayleigh [6], who was able to reproduce the various stages of degradation by heating marble repeatedly in an oven.

At the microscopic level, an evident (and somewhat surprising) effect of temperature changes, even if uniformly distributed throughout the body, is detachment of the calcite grains one from the other. As shown in the scanning electron micrograph of Fig. 2, the grains remain integral after thermal treatment and it simply appears as if the cementing material between them has been degraded. Experimental observations have shown that a temperature increase of just 20–30°C is sufficient to produce partial decohesion of calcite grains [1], which causes the opening of micro-voids and macroscopically results in permanent expansion of the rock. About ten thermal cycles between 20 and 500°C are sufficient to reduce the material to a mono-crystalline powder of integral calcite grains [3,4]. Mechanical actions (i.e. uniform tension or bending) are instead likely to produce intragranular separation, revealed by the sparkling and facetted appearance of the fracture surfaces, which typically results when rupture of the crystals occurs along cleavage planes [3].

Any satisfactory explanation of these phenomena should include consideration of the material's polycrystalline microstructure. Calcite is known to expand on heating much more in the direction of its optical axis than perpendicular to it [7]. The grains' shapes change with temperature and a grain which fits snugly into the mosaic at a given temperature is no longer able to do so when the temperature is varied; this is because the anisotropy directions of individual grains are oriented randomly. The result is a springing apart of contiguous grains, giving rise to a non-zero residual stress state inside the material. On the other hand, when mechanical actions are applied, the sparkling and facetted appearance of the fracture surfaces reveal that the key role is now played by the resistance of the crystals. In fact, although applied forces change grain shapes in the same way as thermal actions (because calcite is also elastically anisotropic), it takes very high stress levels to produce the same strains consequent to just a few degrees' temperature increase [10].

The main aim of the present study is to explain why thermal actions tend to favor decohesion rather than cleavage fracture of single crystals. To this end, the first step is to define and quantify the true stress state that a uniform temperature increase produces both inside the single grains and at their interface. Then, a

0148-9062/99/$ - see front matter
PII: S0148-9062(98)00169-7

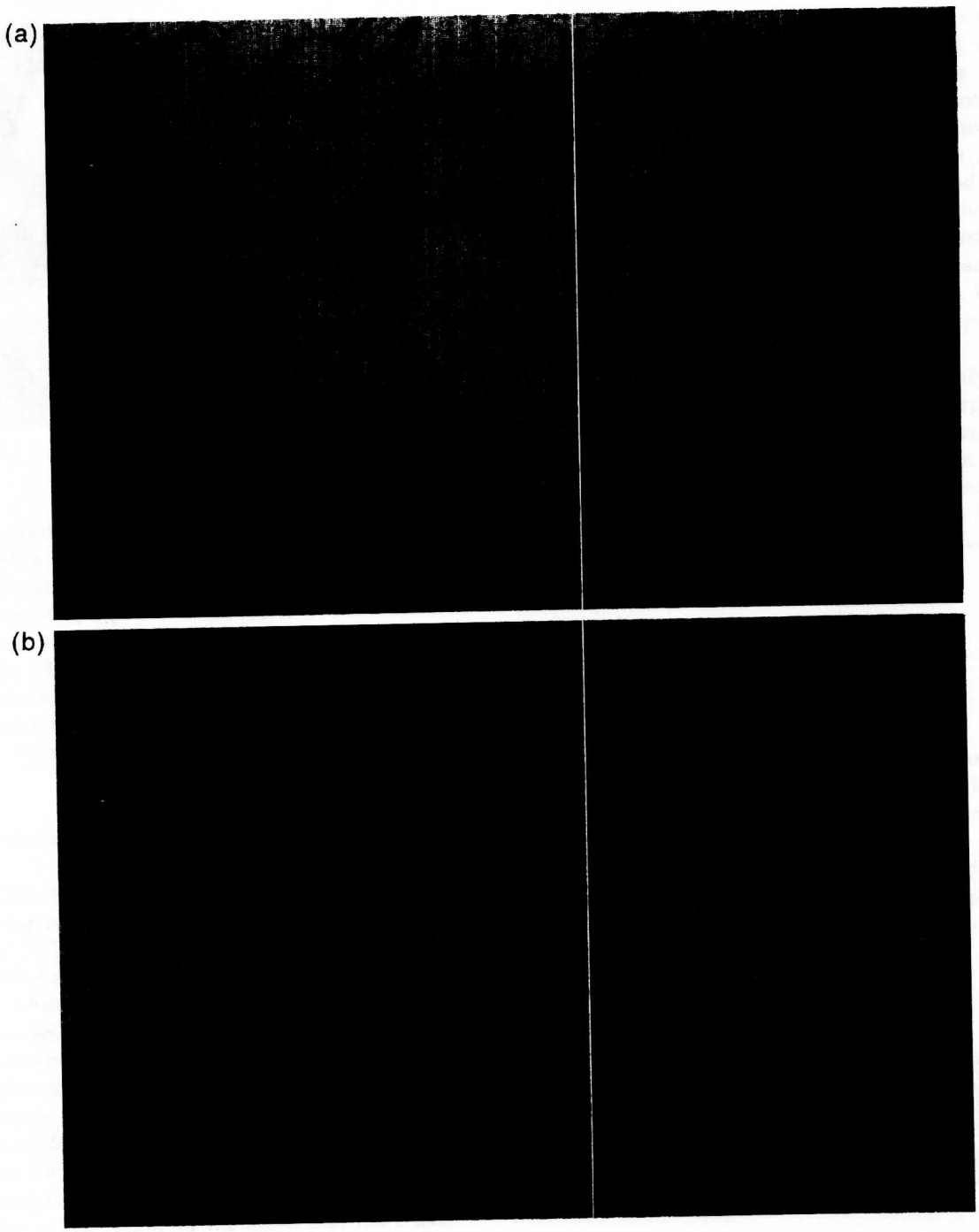

Fig. 1. Typical homoblastic (a) and xenoblastic (b) textures in two different qualities of marble.

further question to be addressed is how marble texture and grain shape might influence the baking phenomenon.

Despite the complexity of the processes involved, a first attempt at qualitative description can be achieved by means of the following model, which takes an averaged view of the phenomena due to the anisotropy of calcite grains and discrepancies in their orientation. Marble is conceived of as an aggregate of grains composed of two elastic phases, both of which (i) are thermally and elastically homogeneous and isotropic; (ii) have equal elastic moduli; (iii) break at the same stress level according to a common failure criterion; (iv) have different coefficients of thermal expansion. A number of approximations have been introduced here. It is clear that, in (i) and (iv), interactions among grains are interpreted by assuming different isotropic thermal expansion coefficients for grains in contact. Secondly,

Fig. 2. Scanning electron micrograph of marble having undergone thermal cycles.

in (ii) the anisotropy of the elastic response is considered to be a secondary effect. Finally, although [9] makes no explicit hypothesis regarding the cementing material between the grains, it is implicit that it must be at least as strong as calcite. It is then clear that intergranular adhesion does not influence the overall response, because failure, if any, would occur in the calcite particles nearest to interfaces, rather than in the thin contact layer between grains.

2. The microstructural model

Fig. 3 offers two examples of grain textures formed by assembling two alternating phases. In Fig. 3(a) the two phases, "a" and "b", are represented by square grains of side l arranged as in a chessboard, "a" occupying the white squares and "b" the black ones. Another possibility is drawn in Fig. 3(b), where the texture is compound of equilateral triangles, each of the sides shared between grains being made up of different phases.

Let us consider a panel of thickness t and diameter D for which we assume $D \gg l \gg t$. We refer the body to a Cartesian coordinate system with the x and y axes placed in the middle plane of the panel and the z axis perpendicular to this plane. Since the panel is thin, we consider a "generalized" plane stress (Ref. [9], art. 8) and the generalized stress components will be unambiguously denoted by σ_{xx}, σ_{yy} and τ_{xy}. Moreover, u_x and u_y indicate the generalized displacements in the x and y directions, respectively, and ϵ_{xx}, ϵ_{yy} and $\epsilon_{xy}=\frac{1}{2}\gamma_{xy}$ the generalized strains. Let E and ν be Young's modulus and Poisson's ratio of both materials and α_a and α_b the coefficients of thermal expansion for materials "a" and "b", respectively. In the absence of body forces and boundary tractions, we aim to find the state of stress due to a uniform temperature increase Δt.

Since each of the grains stretches differently from the others, it is clear that, aside from undergoing a macroscopic dilatation, the body will experience an internal, self-equilibrated state of stress. It will be shown that if $D \gg l$, the complete solution of the elastic problem is the sum of two contributions. The first is given by a hydrostatic stress state, piecewise constant in the panel, yet constant in each grain, of the form

$$\sigma_{xx} = \sigma_{yy} = -\frac{E\Delta t}{1-\nu}\alpha(x, y) + \frac{E\Delta t(\alpha_a + \alpha_b)}{2(1-\nu)}, \qquad \tau_{xy} = 0, \tag{1}$$

where $\alpha(x, y) = \alpha_a$ [or $\alpha(x, y) = \alpha_b$] at points occupied by material "a" (or "b"). The second is the state obtainable by considering the elastic solution corresponding to the problems in Fig. 4(a) [Fig. 4(b)] in each "a" ("b") grain. These are characterized by the mixed boundary conditions: on the grain edges the normal component p of the boundary tractions and

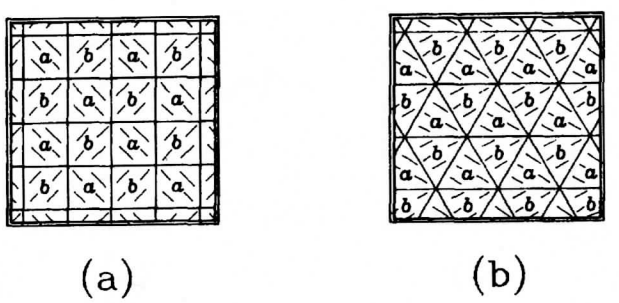

Fig. 3. Examples of grain textures considered by the analysis.

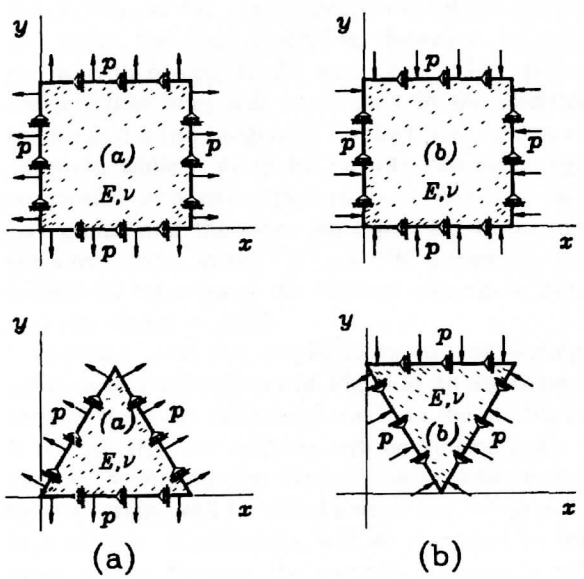

Fig. 4. The reduced schemes for the "periodic additional state" configuration.

the tangential component of displacement are assigned. In particular,

$$p = \frac{E\Delta t(\alpha_a - \alpha_b)}{2(1-\nu)}, \tag{2}$$

and the tangential displacement is equal to zero, as represented by the constraints in Fig. 4. Clearly, the difference in the boundary conditions for "a" and "b" grains consists solely of the sign of the boundary tractions. Note also that when $\alpha_a = \alpha_b$, the model confirms the intuitive expectation that thermal actions do not cause internal stress.

As proof of the previous statement, let us denote as the fundamental state the hypothetical state in which the interfaces between grains, as well as the outer boundary of the panel, are prevented from moving by fictitious restraints as the temperature is raised. In this case, the whole body is clearly in a hydrostatic state of stress, constant piecewise, of the form

$$\sigma_{xx} = \sigma_{yy} = -\frac{E\Delta t}{1-\nu}\alpha(x, y), \quad \tau_{xy} = 0, \tag{3}$$

where the function $\alpha(x, y)$ has been defined in Eq. (1). The complete elastic solution can then be obtained by superimposing onto the fundamental solution an additional state of stress consequent to application of forces equal to, but opposite in sign of those exerted by the fictitious constraints. Thus, in the additional state, the body will be subjected to forces per unit area f, uniformly distributed along the grain interfaces (Fig. 5), of the form

$$f = \frac{E\Delta t(\alpha_a - \alpha_b)}{1-\nu}\mathbf{n}. \tag{4}$$

where $\mathbf{n}$ denotes the unit normal to the interface pointing from material "a" towards material "b". The outer boundary, instead, will be subjected to the tractions given by

$$f^* = \frac{E\Delta t\,\alpha(x, y)}{(1-\nu)}\mathbf{n}^*, \tag{5}$$

with $\mathbf{n}^*$ the outward unit normal to the reference domain of the body and, once again, $\alpha(x, y) = \alpha_a$ or $\alpha(x, y) = \alpha_b$, depending on whether the boundary particles belong to grain type "a" or "b".

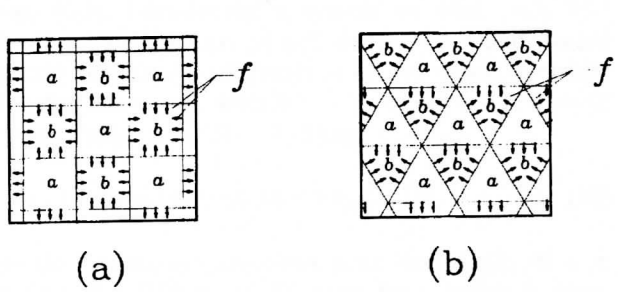

Fig. 5. The additional state configuration.

It is convenient to think of the forces in Eq. (5) as being composed of two parts: the "average" part, given by

$$\overline{f^*} = \frac{E\Delta t(\alpha_a + \alpha_b)}{2(1-\nu)}\mathbf{n}^*, \tag{6}$$

and what will be called the "serrated" part, of the form

$$\tilde{f^*} = (-1)^{h(x,y)}\frac{E\Delta t(\alpha_a - \alpha_b)}{2(1-\nu)}\mathbf{n}^*, \tag{7}$$

where $h(x, y) = 2$ in type "a" grains and $h(x, y) = 1$ in type "b". Clearly, the contribution made by Eq. (6) is a hydrostatic stress state of the form

$$\sigma_{xx} = \sigma_{yy} = \sigma_\infty = \frac{E\Delta t(\alpha_a + \alpha_b)}{2(1-\nu)}, \quad \tau_{xy} = 0. \tag{8}$$

The contribution of Eq. (1) is thus to be interpreted as the sum of Eqs. (3) and (8).

Consider now the remaining part of the "additional state", in which grain interfaces are subjected to the forces per unit area f, given by Eq. (4) and tractions $\tilde{f^*}$ of the form as shown in Eq. (7), acting on the boundary of the body. This condition will be referred to as the "periodic additional state". It may be tentatively assumed that a representative aggregate of grains sufficiently far from the external boundary can be thought of as part of an infinite body. In the case of an infinite body, the interface lines between grains can be considered to be axes of geometrical symmetry. Since thermal actions are not involved in the problem in Fig. 5, the interface lines are also axes of mechanical symmetry because the elastic properties of the grains are the same; the load condition, however, is antisymmetric with respect to the same axes. Thus, points on the interface lines will move only in the direction of the normal $\mathbf{n}$ (no tangential displacement component is allowed), while f, given by Eq. (4), can be thought of as divided into two equal parts, one acting on type "a" grains and the other on type "b". Consequently, the stress states in the "a" and "b" grains can be calculated by referring to the reduced schemes in Fig. 4(a) and (b), with $p = \|f\|/2$.

Examine now the implications of considering the solution to the problems in Fig. 4 as an approximation for the "periodic additional state" in the marble panel. It is clear that the solution will be kinematically compatible throughout the body because deformations of the "a" grains will fit with those of the "b" grains, like in a mosaic. Equilibrium will be respected in the interior grains because the normal tractions p will be provided by the interface forces f given by Eq. (4), while the shear forces due to the reactions of the trans-

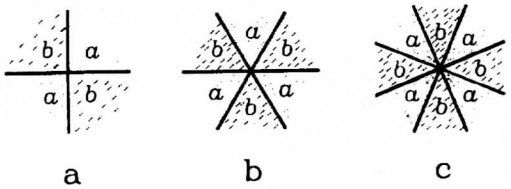

Fig. 6. Examples of connections between the elastic wedges.

3. The stress state at the grain corners

In order to evaluate the state of stress around the grain corners, we imagine magnifying a small region around a texture node in Fig. 3(a) [Fig. 3(b)]. Now the effect of a uniform temperature increase can be regarded as acting in an infinite body composed of four (six) elastic wedges, two (three) made of material "a" and two (three) of material "b", joined together as shown in Fig. 6(a) [Fig. 6(b)]. In general, we will examine the case of connections among, say, n identical wedges of material "a" and the corresponding "n" wedges of "b", arranged alternately as shown in Fig. 6(a), (b) and (c) for $n = 2$, 3 and 4, respectively.

It is again possible to show that complete solution of the elastic problem relative to the schemes in Fig. 6 is given by the sum of the piecewise-constant hydrostatic stress state

$$\sigma_{xx} = \sigma_{yy} = -\frac{E\Delta t}{1-\nu}\alpha(x, y) + \frac{E\Delta t(\alpha_a + \alpha_b)}{2(1-\nu)}, \qquad \tau_{xy} = 0, \tag{12}$$

formally identical to Eq. (1) and that static state obtained by considering problems like those in Fig. 8, with

$$p = \frac{E\Delta t(\alpha_a - \alpha_b)}{2(1-\nu)}. \tag{13}$$

In fact, consider, as before, the fundamental state, characterized by the action of fictitious constraints acting along the interfaces between the wedges and at infinity. The stress state corresponding to this situation is clearly given once again by expressions of the form as shown in Eq. (3). In the additional state the reactions of the fictitious constraints are applied with their signs reversed. Thus, in this second case the straight interfaces between the wedges will be subjected to forces per unit area given by Eq. (4), while at infinity the wedges will be stretched by the tractions

$$f^* = \frac{E\Delta t\,\alpha(x, y)}{1-\nu}\mathbf{n}^*, \tag{14}$$

where $\mathbf{n}^*$ now denotes the outward unit normal to a large circle centered at the vertex of the wedges and $\alpha(x, y)$ has already been defined in Eq. (1).

As before, it is convenient to decompose the tractions in Eq. (14) into their "average" and "serrated" parts, respectively, given by

$$\overline{f^*} = \frac{E\Delta t(\alpha_a + \alpha_b)}{2(1-\nu)}\mathbf{n}^*, \qquad \tilde{f}^* = (-1)^{h(x,y)}\frac{E\Delta t(\alpha_a - \alpha_b)}{2(1-\nu)}\mathbf{n}^*, \tag{15}$$

where $h(x, y) = 2$ [$h(x, y) = 1$] at points occupied by material "a" ("b"). The "average" part contributes with a hydrostatic stress state still of the form as shown in Eq. (8). Summing up the two contributions given by Eqs. (3) and (8), we once again obtain Eq. (12).

The action of the "serrated" boundary tractions (2nd part of Eq. (15)) and of the interface forces (Eq. (4)) will define what has already been called the "*periodic additional state*". This condition is schematically represented in Fig. 7, where

$$q_1 = \frac{E\Delta t(\alpha_a - \alpha_b)}{1-\nu}, \qquad q_2 = \frac{E\Delta t(\alpha_a - \alpha_b)}{2(1-\nu)}. \tag{16}$$

By virtue of symmetry, the problem in Fig. 7 can be reduced to that illustrated in Fig. 8. This represents an infinite elastic wedge defined by the lines $y = 0$ and $y = x\tan\beta$, subjected to mixed-type boundary conditions on the straight edges: the normal tractions are prescribed to be equal to p and no radial displacement components are allowed. In particular,

$$p = q_1/2. \tag{17}$$

From Eqs. (16) and (17), then Eq. (13) follows.

Solutions to the problems in Fig. 8 that satisfy the boundary conditions on the straight edges can be found in explicit form. Introducing a Cartesian coordinate system such that the x axis coincides with one of the straight edges and the wedge lies on the half plane $y > 0$, we first consider the problem illustrated in Fig. 8(a). It can be verified that the constant state of

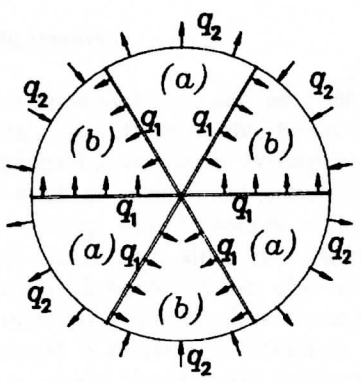

Fig. 7. The "periodic additional state" configuration.

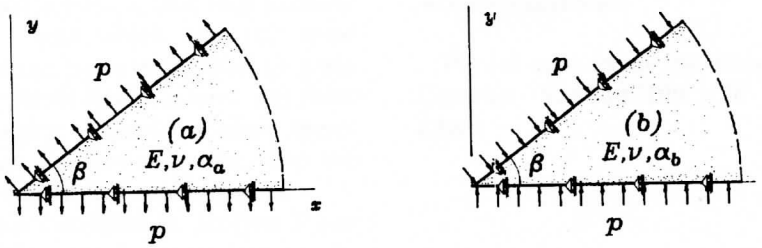

Fig. 8. The reduced scheme for the "additional state" configuration.

stress

$$\sigma_{xx}(x, y) = vp, \qquad \sigma_{yy}(x, y) = p,$$
$$\tau_{xy}(x, y) = -\frac{1-v}{2} p \tan\beta, \tag{18}$$

implies vanishing of the radial displacement along the wedge edges, as well as continuity of the normal tractions with the prescribed value p, provided that $0 < \beta < \pi/2$.

But for $\beta = \pi/2$, we have another stress state, completely different from Eq. (18), of the form

$$\sigma_{xx}(x, y) = p\left[v + \frac{2(1-v)}{\pi}\arctan\frac{y}{x}\right],$$
$$\sigma_{yy}(x, y) = p\left[1 - \frac{2(1-v)}{\pi}\arctan\frac{y}{x}\right], \tag{19}$$
$$\tau_{xy}(x, y) = \frac{1-v}{\pi} p \ln\frac{x^2+y^2}{\lambda^2},$$

where λ is a constant having the dimension of a length. It is also simple to verify that the boundary conditions for the problem of the right-angled sector are satisfied by Eq. (19), whatever the value of λ. This is an undetermined parameter to be correlated with a stress state of the form $\sigma_{xx} = \sigma_{yy} = 0$, $\tau_{xy} = \text{constant} = K$, to which correspond the strains $\varepsilon_{xx} = \varepsilon_{yy} = 0$, $\gamma_{xy} = \text{constant} = K/G$ and a displacement field of the type $(u_x, u_y) = /2G(y, x)$, compatible with the displacement constraints on the straight wedges.

Thus, there is a remarkable difference between the cases $\beta = \pi/n$, with $n \neq 2$ and $\beta = \pi/2$. Let us consider the contribution in Eq. (12) and define a parameter h, such that $h = 1$ ($h = 2$) for wedges made of material "a" ("b"). Then, from Eqs. (13), (18) and (19), the complete stress state becomes

$$\sigma_{xx}(x, y) = (-1)^h \frac{E\Delta t(\alpha_a - \alpha_b)}{2}, \qquad \sigma_{yy}(x, y) = 0,$$
$$\tau_{xy}(x, y) = (-1)^h \frac{E\Delta t(\alpha_a - \alpha_b)}{4}\tan\frac{\pi}{n}, \tag{20}$$

when the connection is among more than four wedges ($n > 2$) and

$$\sigma_{xx}(x, y) = (-1)^h \frac{E\Delta t(\alpha_a - \alpha_b)}{2}\left(1 - \frac{2}{\pi}\arctan\frac{y}{x}\right),$$
$$\sigma_{yy}(x, y) = (-1)^h \frac{E\Delta t(\alpha_a - \alpha_b)}{\pi}\arctan\frac{y}{x}, \tag{21}$$
$$\tau_{xy}(x, y) = -(-1)^h \frac{E\Delta t(\alpha_a - \alpha_b)}{2\pi}\ln\frac{x^2+y^2}{\lambda^2}.$$

when $n = 2$ ($\beta = \pi/2$).

Therefore, the theory predicts constant and finite stress in the wedges, with a stress state that is more favorable the sharper the angle of the corner is and, as the limit case, stress singularities for those textures where the grains are square-shaped.

Instead of thin panels, we could as well consider marble specimens composed of long, prismatic calcite grains under plane strain (Ref. [9], art. 8) that present the same cross-section as the previous case. The corresponding state of stress can now be obtained through expressions similar to those above, i.e. Eqs. (20) and (21), by substituting $E/(1-v^2)$ for E and $(1+v)\alpha_a$ or $(1+v)\alpha_b$ for α_a or α_b, respectively. Specifically therefore, the components of stress σ_{xx}, σ_{yy}, τ_{xy} result $1/(1-v)$ times greater than the quantities corresponding to the plane-stress case, with an increment of about 20% for the appropriate values of Poisson's ratio.

4. Concluding remarks

The model presented here can be used to interpret some important aspects of marble behavior. Since the two-phase material is elastically homogeneous and isotropic, any kind of mechanical action, for example three-point bending, would produce a clearly identifiable state of stress and, since the marble specimen must be considered homogeneous also with regard to failure, the material would break at those points where the limit strength is reached, independent of the grain texture. This explains the cleavage fractures commonly observed in mechanical tests.

A peculiarity of thermal actions is that they produce self-equilibrated stress states which are the most dangerous precisely in those particles located at grain interfaces. It is at these points that fractures will most likely initiate and propagate. Thermal actions, therefore, more often produce decohesion rather than the cleavage fracture of the constituent calcite grains.

Moreover, the problem discussed in Section 3 can clarify how baking is influenced by grain texture. As the angle $\beta = \pi/n$ varies from very small values to $\pi/2$, the connection among the grain apices results more like the homoblastic than the xenoblastic pattern. Xenoblastic textures are, in fact, characterized by sharp corners and deep interlacing of the calcite grains, while the regular homoblastic textures resemble more closely the chessboard arrangement. Therefore, from the theory it can be conjectured that marble with xenoblastic texture is more resistant to baking than the homoblastic varieties. Such theoretical predictions arising from the model have, in fact, been confirmed by experimental trials (see Franzini *et al.* [3–5]).

The current state of many historical monuments clearly reveals that they are not immune to the "baking" action of daily or seasonal temperature changes. The question therefore arises whether certain types of marble are better suited to the maintenance, restoration and construction of such structures. In conclusion, this study suggests, albeit tentatively, that grain texture and, in particular, the average sharpness of the calcite ridges, may be the major qualifying characteristic for selecting marbles able to endure over the years.

Acknowledgements

Partial support of the European Community under Contract SMT4-CT96-2130 is gratefully acknowledged.

References

[1] Battaglia S, Franzini M, Mango F. High sensitivity apparatus for measuring linear thermal expansion: preliminary results on the response of marbles to thermal cycles. Il Nuovo Cimento 1993;16:453–61.

[2] Courant R, Hilbert DM. Methods of Mathematical Physics. New York: J. Wiley and Sons, 1962.

[3] Franzini M. Stones in monuments: natural and anthropogenic deterioration of marble artifacts. Eur. J. Mineral. 1995;7:735–43.

[4] Franzini M, Bertagnini A, Gratziu C, Spampinato M. Il Marmo Cotto in Natura e nei Monumenti. Rendiconti Società Italiana di Mineralogia e Petrografia 1983;39:39–46.

[5] Franzini M, Gratziu C, Spampinato M. Degradazione del Marmo per Effetto di Variazioni di Temperatura. Rendiconti Società Italiana di Mineralogia e Petrografia 1983;39:47–58.

[6] Raileigh A. The bending of marble. Proceeding Royal Society of London 1934;19:266–79.

[7] Rosenholtz JL, Smith DT. Linear thermal expansion of calcite, Var. Iceland Spar, and Yule Marble. Am. Mineral. 1949;34:846–54.

[8] Sternberg E. On Saint-Venant's principle. Q. Appl. Math. 1954;11:393–402.

[9] Timoshenko SP, Goodier JN. Theory of Elasticity. New York: McGraw-Hill, 1970.

[10] Turner FJ, Griggs DT, Heard H. Experimental deformation of calcite crystals. Bull. Geol. Soc. Am. 1954;65:883–934.